PI3K-resistant GSK3 controls adiponectin formation and protects from metabolic syndrome

Hong Chen[a], Abul Fajol[a], Miriam Hoene[b], Bingbing Zhang[a], Erwin D. Schleicher[b,c,d], Yun Lin[e], Carsten Calaminus[e], Bernd J. Pichler[e], Cora Weigert[b,c,d], Hans U. Häring[b,c,d], Florian Lang[a,f], and Michael Föller[a,g,1]

[a]Department of Physiology, University of Tübingen, 72076 Tuebingen, Germany; [b]Division of Clinical Chemistry and Pathobiochemistry, Department of Internal Medicine IV, University Hospital Tübingen, 72076 Tuebingen, Germany; [c]Institute for Diabetes Research and Metabolic Diseases of the Helmholtz-Zentrum München, University of Tübingen, 72076 Tuebingen, Germany; [d]German Center for Diabetes Research, 85764 Neuherberg, Germany; [e]Werner Siemens Imaging Center, Department of Preclinical Imaging and Radiopharmacy, University of Tübingen, 72076 Tuebingen, Germany; [f]Department of Internal Medicine III, University Hospital Tübingen, 72076 Tuebingen, Germany; and [g]Institute of Agricultural and Nutritional Sciences, Martin-Luther University Halle-Wittenberg, D-06120 Halle (Saale), Germany

Edited by Tak W. Mak, The Campbell Family Institute for Breast Cancer Research at Princess Margaret Cancer Centre, University Health Network, Toronto, Canada, and approved April 13, 2016 (received for review January 26, 2016)

Metabolic syndrome is characterized by insulin resistance, obesity, and dyslipidemia. It is the consequence of an imbalance between caloric intake and energy consumption. Adiponectin protects against metabolic syndrome. Insulin-induced signaling includes activation of PI3 kinase and protein kinase B (PKB)/Akt. PKB/Akt in turn inactivates glycogen synthase kinase (GSK) 3, a major regulator of metabolism. Here, we studied the significance of PI3K-dependent GSK3 inactivation for adiponectin formation in diet-induced metabolic syndrome. Mice expressing PI3K-insensitive GSK3 ($gsk3^{KI}$) and wild-type mice ($gsk3^{WT}$) were fed a high-fat diet. Compared with $gsk3^{WT}$ mice, $gsk3^{KI}$ mice were protected against the development of metabolic syndrome as evident from a markedly lower weight gain, lower total body and liver fat accumulation, better glucose tolerance, stronger hepatic insulin-dependent PKB/Akt phosphorylation, lower serum insulin, cholesterol, and triglyceride levels, as well as higher energy expenditure. Serum adiponectin concentration and the activity of transcription factor C/EBPα controlling the expression of adiponectin in adipose tissue was significantly higher in $gsk3^{KI}$ mice than in $gsk3^{WT}$ mice. Treatment with GSK3 inhibitor lithium significantly decreased the serum adiponectin concentration of $gsk3^{KI}$ mice and abrogated the difference in C/EBPα activity between the genotypes. Taken together, our data demonstrate that the expression of PI3K-insensitive GSK3 stimulates the production of adiponectin and protects from diet-induced metabolic syndrome.

obesity | insulin resistance | triglycerides | leptin

Metabolic syndrome is characterized by obesity, adipose tissue accumulation, decreased glucose tolerance with hyperglycemia, dyslipidemia with hypertriglyceridemia, and an elevated low-density lipoprotein (LDL)/ high-density lipoprotein (HDL) ratio, as well as by hypertension (1–3). Millions of patients are affected by this medical condition world-wide and have to face high cardiovascular mortality as its consequence (4, 5). Although the exact mechanisms are still to be elucidated, it appears to be established that metabolic syndrome develops mainly due to an imbalance between caloric intake and needs (6, 7). In particular, the diet of patients with metabolic syndrome is often high in fats, and the patients' lifestyle is characterized by a lack of physical exercise (7, 8). Apart from lifestyle factors, a genetic disposition is also involved (9, 10).

A key process in the development of metabolic syndrome is peripheral insulin resistance (11, 12). In particular, hepatic insulin resistance plays a major role and results in the failure of insulin to suppress hepatic gluconeogenesis (13). Moreover, insulin promotes the uptake of glucose by muscle cells and adipocytes (14, 15). The common consequence of insulin resistance is hyperglycemia and reduced glucose tolerance (11). On the molecular level, binding of insulin to its membrane receptor results in the induction of phosphatidylinositide 3 (PI3) kinase activity, which leads to activation of protein kinase B (PKB)/Akt isoforms, thereby also activating these serine/threonine kinases (12, 16). PKB/Akt is a central mediator of insulin effects in various organs (17). Hence, hepatic insulin resistance can be detected by the failure of insulin to induce PKB/Akt phosphorylation (17, 18). One important molecular target of PKB/Akt is glycogen synthase kinase 3 (GSK3), a serine/threonine kinase (19, 20). Insulin-stimulated PKB/Akt phosphorylates GSK3, thereby rendering this kinase inactive (17). GSK3 is an important cellular regulator of metabolism, but also of cell proliferation, migration, cell death, and immune function (21–24).

To study the physiological relevance of PI3 kinase-dependent inactivation of GSK3, transgenic mice were generated ($gsk3^{KI}$) expressing a mutant GSK3α,β, which cannot be phosphorylated by PKB/Akt. Hence, $gsk3^{KI}$ mice are resistant to the insulin-induced and PI3 kinase-mediated inactivation of GSK3 activity. Surprisingly, $gsk3^{KI}$ mice do not show any signs of type 2 diabetes and are fertile (25). Therefore, the insulin-induced inactivation of GSK3 does not appear to be an absolute prerequisite for proper insulin signaling. However, $gsk3^{KI}$ mice have a lower plasma corticosterone and aldosterone concentration, as well as a higher renal sodium excretion and blood pressure than $gsk3^{WT}$ mice (26). $Gsk3^{KI}$ mice suffer from proteinuria due to glomerular injury, which may be related to their hypertension (27), and from renal calcium and phosphate loss with demineralized bone (28).

Multiple manifestations of the metabolic syndrome are counteracted by the adipose tissue-derived protein hormone adiponectin

Significance

The PI3 kinase-dependent inactivation of glycogen synthase kinase (GSK) 3 is an important aspect of normal insulin signaling. Surprisingly, transgenic mice expressing PI3 kinase-resistant GSK3 ($gsk3^{KI}$) have been found not to be insulin-resistant. We show that $gsk3^{KI}$ mice are even protected from the development of metabolic syndrome characterized by insulin resistance, obesity, and dyslipidemia, which all could readily be induced by a high-fat diet in $gsk3^{WT}$ mice. The metabolic syndrome affects millions of patients and is associated with a high prevalence of cardiovascular disease and a significant reduction of life span. Exploring the underlying mechanism, we found that the production of the hormone adiponectin, which provides protection from metabolic syndrome, is controlled by a GSK3-dependent pathway.

Author contributions: F.L. and M.F. designed research; H.C., A.F., M.H., B.Z., and Y.L. performed research; H.C., M.H., E.D.S., C.C., B.J.P., C.W., H.U.H., and M.F. analyzed data; and H.C. and M.F. wrote the paper.

The authors declare no conflict of interest.

This article is a PNAS Direct Submission.

[1]To whom correspondence should be addressed. Email: michael.foeller@landw.uni-halle.de.

This article contains supporting information online at www.pnas.org/lookup/suppl/doi:10.1073/pnas.1601355113/-/DCSupplemental.

(29–33). The hormone thus protects against the development of type II diabetes and hyperglycemia by improving insulin sensitivity (34, 35). Moreover, it ameliorates dyslipidemia by lowering the serum triglyceride concentration (36) and favoring the formation of HDL-cholesterol (37). In line with its beneficial effects, a low serum adiponectin concentration is associated with metabolic syndrome (38). Adiponectin may therefore be a valuable biomarker for metabolic syndrome.

Here, we studied the significance of the PI3 kinase-dependent inactivation of GSK3 for the development of insulin resistance, decreased glucose tolerance, obesity, and dyslipidemia in a mouse model of diet-induced metabolic syndrome. Moreover, we characterized the role of GSK3 in the formation of the hormone adiponectin.

Results

We compared mice expressing a mutant GSK3α,β, in which the codon encoding Ser9 of the GSK3β gene was changed to encode nonphosphorylable alanine ($GSK3\beta^{9A/9A}$), and simultaneously the codon encoding Ser21 of GSK3α was changed to encode the nonphosphorylable $GSK3\alpha^{21A/21A}$ ($gsk3^{KI}$) to wild-type mice ($gsk3^{WT}$). Metabolic syndrome can be induced by feeding the mice a high-fat diet (39). We first monitored the weight gain of the mice on this diet. Compared with $gsk3^{WT}$ mice, the weight gain was considerably smaller in $gsk3^{KI}$ mice (Fig. 1*A*). Hence, at 11 wk, the relative weight gain was significantly higher in $gsk3^{WT}$ mice than in $gsk3^{KI}$ mice (Fig. 1*B*).

Feeding the high-fat diet increases body weight due to expansion of adipose tissue. Therefore, we analyzed the adipose tissue distribution of these mice on control diet and on high-fat diet. As illustrated in Fig. 1 *C* and *D*, no significant differences were observed on control diet whereas the mass of subcutaneous, mesenteric, epididymal, and perirenal adipose tissue was significantly larger in $gsk3^{WT}$ mice than in $gsk3^{KI}$ mice on high-fat diet. In line with a higher fat mass, the serum level of the adipose tissue-derived hormone leptin was dramatically higher in $gsk3^{WT}$ mice than in $gsk3^{KI}$ mice on a high-fat diet (Fig. 1*E*). Moreover, the high-fat diet induced hepatic steatosis (fatty liver) in $gsk3^{WT}$ mice but failed to do so in $gsk3^{KI}$ mice (Fig. 1 *F* and *G*).

Another hallmark of metabolic syndrome is dyslipidemia characterized by high serum levels of triglycerides (hypertriglyceridemia) and a high LDL/HDL ratio indicative of a low HDL-cholesterol serum concentration (1, 40). We therefore analyzed the blood lipids in $gsk3^{WT}$ mice and $gsk3^{KI}$ mice. Following 7–8 wk of feeding the mice the high-fat diet, the serum triglyceride (Fig. 2*A*) and total cholesterol (Fig. 2*B*) levels were markedly higher in $gsk3^{WT}$ mice than in $gsk3^{KI}$ mice. Moreover, both the HDL-cholesterol and LDL-cholesterol serum concentrations were higher in $gsk3^{WT}$ mice than in $gsk3^{KI}$ mice on control and high-fat diet (Fig. 2*C*). When maintained on control diet, the LDL/HDL ratio was not different between the genotypes (Fig. 2*D*). However, feeding a high-fat diet resulted in a much stronger increase in the serum level of LDL-cholesterol in $gsk3^{WT}$ mice than in $gsk3^{KI}$ mice. Therefore, the LDL/HDL ratio in high-fat-diet–fed $gsk3^{WT}$ mice was significantly higher than that in $gsk3^{KI}$ mice (Fig. 2*D*).

Metabolic syndrome affects glucose metabolism and results in peripheral insulin resistance, lower glucose tolerance, and hyperglycemia (11, 41). We therefore analyzed the blood glucose concentration in fasted $gsk3^{WT}$ mice and $gsk3^{KI}$ mice maintained for 10 wk on a high-fat diet. Compared with $gsk3^{KI}$ mice, $gsk3^{WT}$ mice were markedly hyperglycemic (Fig. 3*A*), suggesting that the high-fat diet induced insulin resistance. To test this possibility, we first carried out a glucose tolerance test. Fig. 3*B* demonstrates that glucose tolerance was greatly reduced in $gsk3^{WT}$ mice fed a high-fat diet for 10 wk compared with $gsk3^{KI}$ mice on the same diet. In contrast, glucose tolerance was similar in $gsk3^{WT}$ mice and $gsk3^{KI}$ mice on control diet with significantly lower blood glucose concentrations in $gsk3^{KI}$ mice only at 0 and 15 min of the glucose tolerance test (Fig. S1*A*). Next, we determined the circulating insulin concentration of fasted and unfasted mice on a high-fat diet. As expected, fasted $gsk3^{WT}$ mice exhibited hyperinsulinemia in comparison with $gsk3^{KI}$ mice (Fig. 3*C*), suggesting decreased insulin sensitivity as the main cause of glucose intolerance in $gsk3^{WT}$ mice. The serum insulin concentration, however, was not significantly different between unfasted $gsk3^{WT}$ and $gsk3^{KI}$ mice (Fig. 3*C*). We did not observe a significant difference between the circulating glucagon levels in fasted $gsk3^{WT}$ mice and $gsk3^{KI}$ mice either (Fig. 3*D*). Glucose-induced insulin secretion was significantly stronger in high-fat-diet–fed $gsk3^{WT}$ mice compared with $gsk3^{KI}$ mice, again pointing to reduced insulin sensitivity of $gsk3^{WT}$ mice (Fig. 3*E*). To further characterize the responsiveness of $gsk3^{WT}$ mice and $gsk3^{KI}$ mice to insulin (17), we determined P-Akt (Thr308) in liver tissue isolated

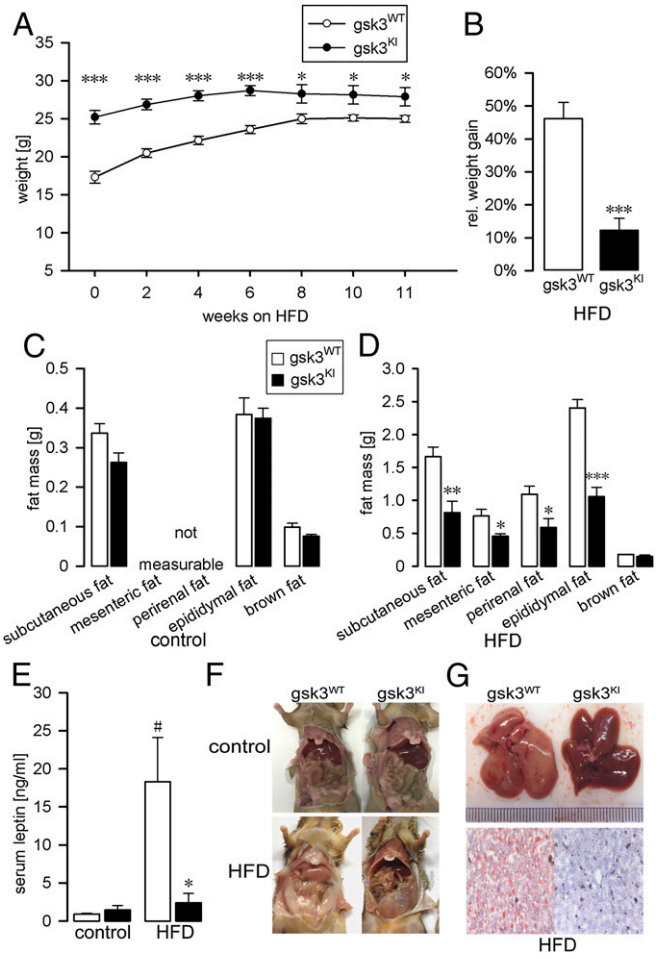

Fig. 1. High-fat-diet–induced obesity and fat accumulation in $gsk3^{WT}$ mice but not in $gsk3^{KI}$ mice. Body weight (*A*; $n = 9$) in dependence on the duration of high-fat-diet feeding (HFD), relative weight gain after 11 wk of high-fat-diet feeding (*B*; $n = 9$), the mass of different fat depots of 6-mo-old mice on control diet (*C*; $n = 5$) and of 6-mo-old mice after 4 mo of high-fat-diet feeding (*D*, $n = 4$), and the serum leptin concentration (*E*; $n = 5$–6) before (control) and after 10 wk of high-fat-diet feeding. All parameters were determined in $gsk3^{WT}$ mice (white bars) and $gsk3^{KI}$ mice (black bars) and are given as arithmetic means ± SEM. (*F* and *G*) High-fat-diet feeding induced fatty liver in $gsk3^{WT}$ mice but not in $gsk3^{KI}$ mice. Shown is the abdominal situs of mice (*F*) on control diet (*Upper* panels) and high-fat diet (*Lower* panels); in addition, the livers and a microphotograph (*G*) of Oil Red O staining to visualize lipid droplets of hepatic sections is demonstrated. (Magnification: ×200.) (*Left* panels) $gsk3^{WT}$ mice. (*Right* panels) $gsk3^{KI}$ mice. $^{*}P < 0.05$, $^{**}P < 0.01$, and $^{***}P < 0.001$ indicate significant difference between the genotypes; $^{\#}P < 0.05$ indicates significant difference from the absence of HFD treatment.

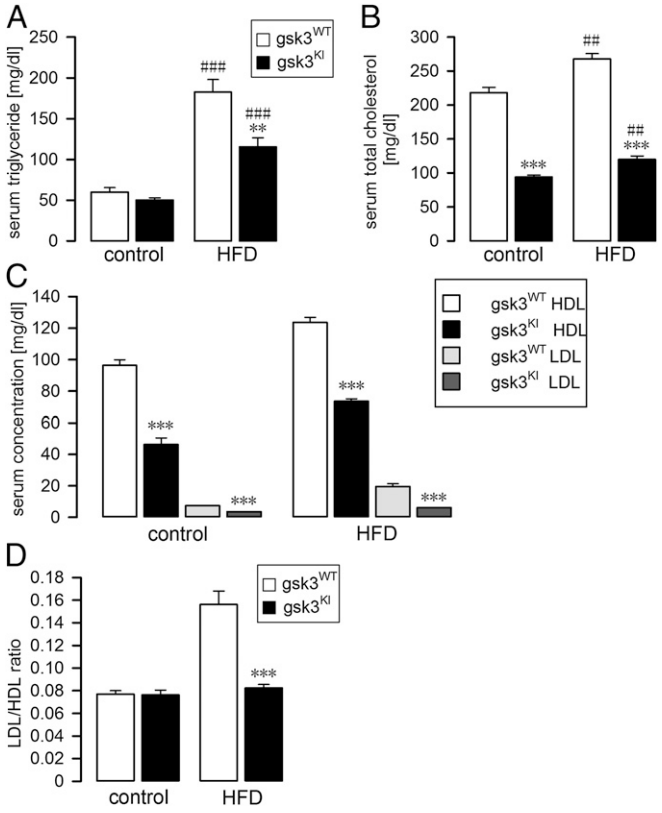

Fig. 2. High-fat-diet–induced dyslipidemia in gsk3^{WT} mice but not in gsk3^{KI} mice. Serum triglyceride (*A*; $n = 6$–7) and total cholesterol concentration (*B*; $n = 6$) before (control) and after 7–8 wk of feeding a HFD. HDL- and LDL-cholesterol concentrations (*C*; $n = 5$–6) and LDL/HDL ratio (*D*; $n = 5$–7) of 3- to 4-mo-old mice on control diet and of 3- to 4-mo-old mice on HFD for 7–8 wk. All parameters were determined in gsk3^{WT} mice (white bars) and gsk3^{KI} mice (black bars) and are given as arithmetic means ± SEM. $^{**}P < 0.01$ and $^{***}P < 0.001$ indicate significant difference between the genotypes. $^{\#\#}P < 0.05$ and $^{\#\#\#}P < 0.001$ indicate significant difference from the absence of HFD treatment.

from the mice 8 min after insulin injection. As illustrated in Fig. 3*F*, following the injection of insulin the abundance of P-Akt (Thr308) was markedly and significantly higher in hepatic tissue from gsk3^{KI} mice compared with gsk3^{WT} mice whereas total Akt abundance was not different between the genotypes (Fig. 3*G*). This result further demonstrates that the high-fat diet resulted in peripheral insulin resistance in gsk3^{WT} mice but not in gsk3^{KI} mice. On control diet, hepatic insulin-induced Akt phosphorylation was not significantly different between the genotypes. (Fig. S1 *B* and *C*).

Phosphatase PTEN is regulated by phosphorylation at Ser380/Thr382/383 and counteracts PI3K-mediated signaling. PTEN phosphorylation was not significantly different in the livers from high-fat-diet–fed gsk3^{KI} and gsk3^{WT} mice (Fig. S2 *A* and *B*).

Thus far, our data indicate that gsk3^{KI} mice are protected from the development of metabolic syndrome (41), characterized by obesity, adipose tissue accumulation, dyslipidemia, and peripheral glucose intolerance, which all were readily induced by a high-fat diet in gsk3^{WT} mice. The adipose tissue-derived hormone adiponectin has been shown to provide protection against these manifestations of metabolic syndrome (29, 42). We therefore determined the serum adiponectin level in gsk3^{KI} mice and gsk3^{WT} mice. As illustrated in Fig. 4*A*, the serum adiponectin concentration was significantly higher in gsk3^{KI} mice compared with gsk3^{WT} mice both before and after feeding of the high-fat diet. The stimulation of energy consumption contributes to the effects of adiponectin protecting against the development of metabolic syndrome (43). Thus, we measured energy expenditure in gsk3^{KI} mice and gsk3^{WT} mice. In line with their high serum adiponectin level, we found significantly higher energy expenditure in gsk3^{KI} mice compared with gsk3^{WT} mice (Fig. 4*B*).

The main regulator of adiponectin formation in adipose tissue is transcription factor C/EBPα (44). GSK3 has been shown to regulate C/EBPα (45). We therefore determined the activity of C/EBPα in adipose tissue from gsk3^{KI} mice and gsk3^{WT} mice by Western blotting. As demonstrated in Fig. 5*A*, the abundance of P-C/EBPα (Thr222/226) was significantly higher in adipose tissue from gsk3^{KI} mice compared with gsk3^{WT} mice, pointing to enhanced

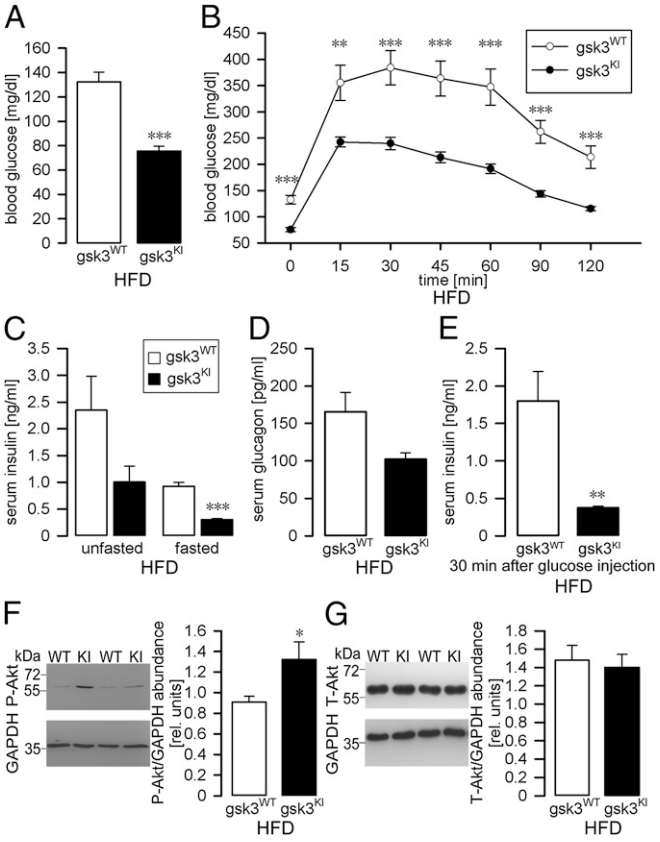

Fig. 3. High-fat-diet–induced hyperglycemia, glucose intolerance, and insulin resistance in gsk3^{WT} mice but not in gsk3^{KI} mice. Arithmetic means ± SEM of the fasted blood glucose level (*A*; $n = 11$–13) and of the blood glucose concentration (*B*; $n = 11$–13) following i.p. injection of glucose (2 g/kg body weight) into fasted gsk3^{WT} and gsk3^{KI} mice. (*C*) Circulating insulin levels. Arithmetic means ± SEM of the serum insulin concentration ($n = 5$–6) of gsk3^{WT} and gsk3^{KI} mice; the animals were fasted overnight (*Right* bars) or unfasted (*Left* bars) right before the experiment. (*A*–*C*) All mice had been maintained for 10 wk on a HFD. (*D*) Circulating glucagon levels. Arithmetic means ± SEM of the serum glucagon concentration ($n = 6$–7) of gsk3^{WT} and gsk3^{KI} mice; all mice had been maintained for 8 wk on a high-fat diet and were fasted overnight right before the experiment. (*E*) Glucose-induced insulin secretion. Arithmetic means ± SEM of the serum insulin concentration ($n = 5$–6) 30 min after i.p. glucose injection (2 g/kg body weight) into gsk3^{WT} and gsk3^{KI} mice; all mice had been maintained for 10 wk on a high-fat diet and were fasted overnight right before the experiment. (*F* and *G*) Original Western blots (*Left* panels) demonstrating the abundance of P-Akt (Thr308, *F*) and total Akt (*G*) in livers isolated from gsk3^{WT} and gsk3^{KI} mice 8 min after insulin injection (0.5 U/kg body weight). The mice had been fed a high-fat diet for 12 wk. GAPDH expression is also shown. (*Right* panels) Densitometric analysis (arithmetic means ± SEM; $n = 4$–7); white bars: gsk3^{WT} mice; black bars: gsk3^{KI} mice. $^{*}P < 0.05$, $^{**}P < 0.01$, and $^{***}P < 0.001$ indicate significant difference from gsk3^{WT} mice.

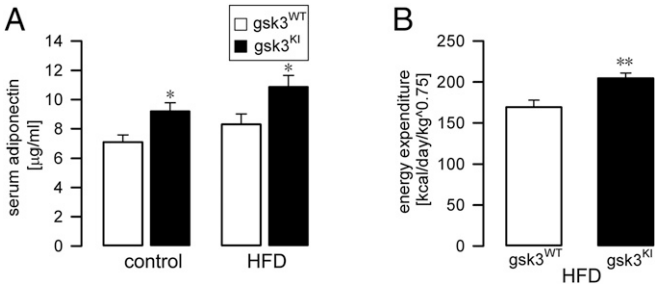

Fig. 4. Gsk3^{KI} mice on a high-fat diet exhibited a higher serum adiponectin level and energy expenditure. (*A*) Arithmetic means ± SEM of the serum adiponectin concentration (n = 9–11) in gsk3^{WT} mice (white bars) and gsk3^{KI} mice (black bars) before (control) and after 9–10 wk of feeding a HFD. (*B*) Arithmetic means ± SEM of energy expenditure (n = 6) in gsk3^{WT} mice (white bar) and gsk3^{KI} mice (black bar) determined after 10–11 wk of feeding a high-fat diet. *P < 0.05 and **P < 0.01 indicate significant difference from gsk3^{WT} mice.

C/EBPα activity in gsk3^{KI} mice. Total C/EBPα was not different between the genotypes (Fig. 5*B*).

As a last step, we treated gsk3^{KI} mice and gsk3^{WT} mice with GSK3 inhibitor lithium chloride to test whether GSK3 kinase activity accounted for enhanced adiponectin formation in gsk3^{KI} mice. We found that a 21-d treatment with lithium significantly lowered the serum adiponectin concentration in gsk3^{KI} mice but not in gsk3^{WT} mice (Fig. 6*A*). Upon treatment with lithium chloride, no difference in P-C/EBPα (Thr222/226) abundance in adipose tissue from gsk3^{KI} mice and gsk3^{WT} mice could be found, indicating similar C/EBPα activity after inhibition of GSK3 (Fig. 6 *B* and *C*). The hepatic abundance of P-Akt (Thr308) and total Akt was not different between lithium-chloride–treated gsk3^{KI} mice and gsk3^{WT} mice either (Fig. 6 *D* and *E*).

Discussion

Our study reveals that the PI3 kinase-dependent inhibition of GSK3 is an important regulator of adiponectin formation. Mice expressing PI3 kinase-resistant GSK3 (gsk3^{KI}) were protected against the development of metabolic syndrome readily induced by feeding a high-fat diet in gsk3^{WT} mice.

As described by others before (46), feeding a high-fat diet caused multiple manifestations of the metabolic syndrome in gsk3^{WT} mice within 12 wk: Gsk3^{WT} mice developed obesity with massive adipose tissue accumulation and fatty liver, dyslipidemia with hypertriglyceridemia, hypercholesterolemia, and high LDL/HDL ratio, as well as hyperglycemia with decreased glucose tolerance and insulin resistance. All these health problems were markedly lower or even absent in gsk3^{KI} mice.

A key process in the development of the metabolic syndrome is hepatic steatosis and insulin resistance (11, 47–49). In our study, we identified hepatic steatosis by oil red staining and insulin resistance by the abundance of phosphorylated PKB/Akt 8 min after insulin injection. Whereas gsk3^{KI} mice were again protected against these manifestations of the metabolic syndrome, gsk3^{WT} mice developed massive hepatic steatosis and insulin resistance.

In an effort to identify the reason for the striking protection of gsk3^{KI} mice against the metabolic syndrome, we showed that the production of the hormone adiponectin is enhanced in gsk3^{KI} mice. In line with low adiponectin serum levels in metabolic syndrome, the serum level of this hormone was significantly higher in gsk3^{KI} mice compared with gsk3^{WT} mice. Moreover, because GSK3 inhibitor lithium reduced adiponectin production in gsk3^{KI} mice, it appears safe to conclude that, indeed, GSK3 activity accounted for its enhanced formation. Notably, lithium has recently been shown to lower the serum adiponectin concentration in patients treated with this drug for bipolar disorders (50). Our study now sheds light on the underlying mechanism, i.e., lithium-dependent inhibition of GSK3.

Adiponectin has been demonstrated to counteract the development of metabolic syndrome (29) and to be particularly effective against insulin resistance (51, 52). Therefore, we conclude that enhanced adiponectin formation contributes to the observed resistance of gsk3^{KI} mice to diet-induced metabolic syndrome. We also elucidated the underlying mechanism: GSK3 phosphorylates the transcription factor C/EBPα at Thr226/222 (45). C/EBPα is the key transcription factor required for the production of adiponectin (44, 53). In line with a decisive role of GSK3 in the control of C/EBPα activity, treatment with GSK3 inhibitor lithium chloride abrogated the difference in C/EBPα phosphorylation between the genotypes. Our study therefore discloses GSK3 as a major regulator of adiponectin formation in adipose tissue.

Adiponectin deficiency favors not only metabolic syndrome, but also the development of typical sequelae such as atherosclerosis, coronary heart disease, inflammation, and even some forms of cancer (54–57). Therefore, efforts are undertaken to elucidate the signaling of adiponectin production and to generate agonists of the adiponectin receptor (58). Our results suggest that activation of GSK3 may be a promising way to enhance the serum adiponectin level and to combat metabolic syndrome. On the other hand, several GSK3 inhibitors are currently being developed and tested for the treatment of Alzheimer's disease (59, 60). In view of the present observations, those substances may share with lithium (50) the negative influence on serum adiponectin levels, potentially leading to a negative cardiovascular safety profile (55, 61). Clearly, further research is needed to analyze the impact of GSK3-dependent adiponectin production on the adverse effects of GSK3 inhibitors.

Normal insulin signaling involves the PKB/Akt-dependent phosphorylation of GSK3 (16, 62). This phosphorylation cannot occur in gsk3^{KI} mice. Therefore, it was a surprise that gsk3^{KI} mice are not diabetic (25). Our study now demonstrates that gsk3^{KI} mice are even protected against the development of diabetes, which was readily induced by a high-fat diet in gsk3^{WT} mice. We could not detect significant differences in glucagon production, which could also have contributed to differences in glucose metabolism in gsk3^{KI} mice.

Metabolic syndrome favors the development of different types of cancer (63). PI3K signaling is activated in diverse tumors (64). Hence, PI3K inhibition is therefore considered a promising therapeutic target in cancer (64). Also inhibition of GSK3 has been proposed for cancer therapy (65–67). At least in theory, the beneficial effect of PI3K-insensitive GSK3 on metabolic syndrome

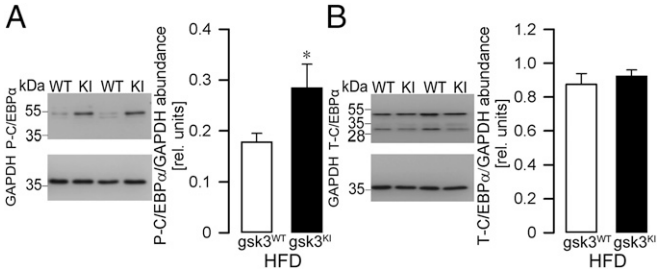

Fig. 5. Higher activity of transcription factor C/EBPα in adipose tissue from gsk3^{KI} mice. Original Western blots demonstrating (*A*) P-C/EBPα (Thr222/226) and GAPDH abundance or (*B*) total C/EBPα and GAPDH abundance (*Left* panels) in epididymal fat tissue from gsk-3^{WT} mice and gsk-3^{KI} mice after 12 wk of feeding a HFD. (*Right* panels) Densitometric analysis (arithmetic means ± SEM; n = 8–15); white bars: gsk3^{WT} mice; black bars: gsk3^{KI} mice. *P < 0.05 indicates significant difference from gsk3^{WT} mice.

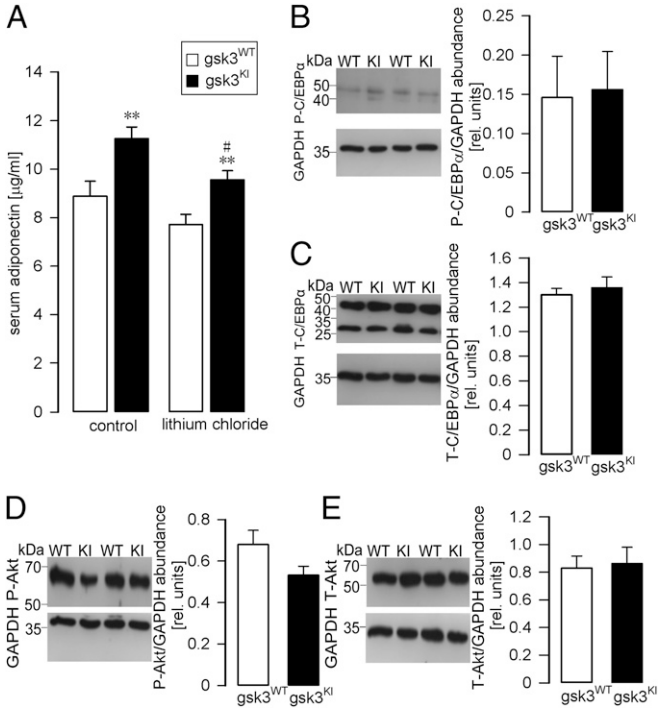

Fig. 6. GSK3 inhibitor lithium lowered the higher serum adiponectin level in gsk3^{KI} mice. (*A*) Arithmetic means ± SEM ($n = 7$) of the serum adiponectin concentration in gsk3^{WT} mice (white bars) and gsk3^{KI} mice (black bars) determined before (*Left* bars) and after 3 wk of oral treatment with lithium chloride (*Right* bars). (*B* and *C*) Original Western blots (*Left* panels) demonstrating (*B*) P-C/EBPα (Thr222/226) and (*C*) total C/EBPα expression in epididymal fat tissue from gsk-3^{WT} mice and gsk-3^{KI} mice after 3 wk of oral treatment with lithium chloride. (*D* and *E*) Original Western blots (*Left* panels) demonstrating the abundance of P-Akt (Thr308, *D*) and total Akt (*E*) in livers isolated from gsk3^{WT} and gsk3^{KI} mice after 3 wk of oral treatment with lithium chloride. For all blots GAPDH expression is also shown. (*Right* panels) Densitometric analysis (arithmetic means ± SEM; $n = 4$); white bars: gsk3^{WT} mice; black bars: gsk3^{KI} mice. $^{**}P < 0.01$ indicates significant difference between the genotypes; $^{\#}P < 0.05$ indicates significant difference from control.

may also be relevant for the growth of tumors. The phosphorylation of PTEN, which negatively regulates downstream PI3K signaling, thereby controlling it, was not different between the genotypes. Clearly, further studies addressing the role of GSK3-associated protection against metabolic syndrome and other diseases associated with deranged PI3K signaling, such as cancer, are warranted.

In conclusion, PI3 kinase/PKB/Akt-sensitive GSK3 signaling is a powerful regulator of adiponectin formation. Thus, transgenic mice expressing PI3 kinase-resistant GSK3 (gsk3^{KI}) are protected from diet-induced metabolic syndrome due to enhanced adiponectin production.

Materials and Methods

Animals and Treatments. All animal experiments were conducted according to the German law for the welfare of animals and were approved by the authorities of the state of Baden-Württemberg. For our study, mice were used, in which the codon encoding Ser9 of the GSK3β gene had been changed to encode nonphosphorylable alanine (GSK3β$^{9A/9A}$) and simultaneously the codon encoding Ser21 of GSK3α had been changed to encode the nonphosphorylable GSK3α$^{21A/21A}$, thus yielding the GSK3α/β$^{21A/21A/9A/9A}$ double knockin mouse (gsk3^{KI}) as already described (25). The mice were kindly provided by Dario Alessi (University of Dundee, Dundee, UK). Only male mice were used in this study. The mice were compared with age-matched wild-type mice (gsk3^{WT}).

At the age of 6–8 wk, mice were fed a high-fat diet containing 70% kcal from fat (Altromin), and body weight was recorded weekly. Control groups were maintained on normal chow (SSniff). All animals had free access to food and tap water. For some experiments, 4-mo-old male mice were maintained on normal chow and in addition were treated with lithium chloride (Roth) in drinking water at a concentration of 600 mg/L for 3 wk as indicated in Fig. 6. Serum was taken 1 wk before and on the last day of the treatment.

For the quantification of the adipose tissue distribution, the mice were killed, and the different depots were weighed.

Blood and Serum Parameters. Animals were lightly anesthetized, and blood from the retro-orbital plexus was collected into serum tubes. Serum leptin, adiponectin, insulin, and glucagon were determined by commercially available ELISA kits from Merck Millipore (leptin and adiponectin), from Crystal Chem (insulin), and from R&D systems (glucagon) according to the manufacturer's instructions. Serum total cholesterol and triglyceride levels were determined by a photometric method according to the manufacturer's instructions (dri-chem clinical chemistry analyzer FUJI FDC 3500i; Sysmex). Serum HDL-cholesterol and LDL-cholesterol were measured by the central laboratory of the University Hospital of Tübingen according to routine clinical chemistry methods (Siemens). The blood glucose concentration was determined in a drop of tail blood by a glucometer (Accu-Chek Performa, Roche).

Glucose Tolerance Test. Glucose (2 g/kg body weight) was injected intraperitoneally (i.p.). The blood glucose concentration was determined in a blood drop from the tail vein before as well as 15, 30, 45, 60, 90, and 120 min after the injection with a glucometer.

Indirect Calorimetry. Energy expenditure was measured using an indirect calorimetric system (Oxylet, Panlab). Mice were individually placed in air-tight metabolic cages (Panlab) and allowed free access to chow and water. Relative energy expenditure was calculated using the Metabolism 2.1.04 Software (Panlab).

Histology. After the mice were killed, the livers were collected immediately, fixed overnight in 4% (vol/vol) paraformaldehyde, snap-frozen in OCT Tissue-Tek (Sakura Finetek), and cut into 8-µm-thick sections. To visualize lipids, the sections were stained with Oil Red O.

Western Blotting. Livers and epididymal fat were collected and immediately shock-frozen in liquid nitrogen. The tissues were then lysed in lysis buffer [54.6 mM 4-(2- hydroxyethyl)-1-piperazineethanesulfonic acid (Hepes); 2.69 mM $Na_4P_2O_7$; 360 mM NaCl; 10% (vol/vol) glycerol and 1% (vol/vol) Nonidet P-40] or RIPA lysis buffer (Cell Signaling Technology), containing phosphatase and protease inhibitor mixture tablets (Complete mini; Roche). After incubation on ice for 30 min and centrifugation at 10,000 × *g* and 4 °C for 20 min, the supernatant was removed and used for Western blotting. Total protein (40 µg) was separated by SDS/PAGE, transferred to PVDF membranes, and blocked in 5% nonfat milk with Tris-buffered saline-Tween-20 (TBST) at room temperature for 1 h. Membranes were probed overnight at 4 °C with rabbit anti-phospho-Akt (Thr308) or -total-Akt antibody with rabbit anti-phospho-C/EBPα (Thr222/226) or -total-C/EBPα antibody, with rabbit anti-phospho-PTEN (Ser380/Thr382/383) or -total-PTEN antibody (all: 1:1,000 in 5% BSA in TBST, Cell Signaling Technology), or with anti-GAPDH antibody (Cell Signaling; 1:2,000 in 5% BSA in TBST) as a loading control. The membranes were washed several times and again incubated with horseradish-peroxidase–conjugated anti-rabbit secondary antibody (1:2,000; Cell Signaling Technology) for 1 h at room temperature. The membranes were washed again, and the bands were visualized with ECL reagents (GE Healthcare-Amersham). The blots were densitometrically analyzed with Quantity One software (Bio-Rad).

Statistics. Data are provided as means ± SEM; *n* represents the number of independent experiments. All data were tested for significance using unpaired Student *t* test. Only results with $P < 0.05$ were considered statistically significant.

ACKNOWLEDGMENTS. The authors acknowledge the technical assistance of E. Faber and thank Dario Alessi for providing the mice used in this study. The study was supported by the Deutsche Forschungsgemeinschaft Grants (Fo 695/1-1, Fo 695/2-1, La 315/15-1, and GRK 1302) in part by grants from the German Federal Ministry of Education and Research (BMBF) to the German Centre for Diabetes Research e.V. Grant (01GI0925), and by the Landesgraduiertenförderung of the state of Baden-Württemberg.

1. Grundy SM, et al. (2006) Diagnosis and management of the metabolic syndrome: An American Heart Association/National Heart, Lung, and Blood Institute scientific statement. *Curr Opin Cardiol* 21(1):1–6.
2. Huang PL (2009) A comprehensive definition for metabolic syndrome. *Dis Model Mech* 2(5-6):231–237.
3. Kassi E, Pervanidou P, Kaltsas G, Chrousos G (2011) Metabolic syndrome: Definitions and controversies. *BMC Med* 9:48.
4. Povel CM, et al. (2013) Metabolic syndrome model definitions predicting type 2 diabetes and cardiovascular disease. *Diabetes Care* 36(2):362–368.
5. Saely CH, et al. (2005) The metabolic syndrome, insulin resistance, and cardiovascular risk in diabetic and nondiabetic patients. *J Clin Endocrinol Metab* 90(10):5698–5703.
6. Wilson PW, D'Agostino RB, Parise H, Sullivan L, Meigs JB (2005) Metabolic syndrome as a precursor of cardiovascular disease and type 2 diabetes mellitus. *Circulation* 112(20):3066–3072.
7. Pitsavos C, Panagiotakos D, Weinem M, Stefanadis C (2006) Diet, exercise and the metabolic syndrome. *Rev Diabet Stud* 3(3):118–126.
8. Edwardson CL, et al. (2012) Association of sedentary behaviour with metabolic syndrome: A meta-analysis. *PLoS One* 7(4):e34916.
9. Ussar S, et al. (2015) Interactions between gut microbiota, host genetics and diet modulate the predisposition to obesity and metabolic syndrome. *Cell Metab* 22(3): 516–530.
10. Chen YW, Harris RA, Hatahet Z, Chou KM (2015) Ablation of XP-V gene causes adipose tissue senescence and metabolic abnormalities. *Proc Natl Acad Sci USA* 112(33): E4556–E4564.
11. Roberts CK, Hevener AL, Barnard RJ (2013) Metabolic syndrome and insulin resistance: Underlying causes and modification by exercise training. *Compr Physiol* 3(1):1–58.
12. Wilcox G (2005) Insulin and insulin resistance. *Clin Biochem Rev* 26(2):19–39.
13. Meshkani R, Adeli K (2009) Hepatic insulin resistance, metabolic syndrome and cardiovascular disease. *Clin Biochem* 42(13-14):1331–1346.
14. Dimitriadis G, Mitrou P, Lambadiari V, Maratou E, Raptis SA (2011) Insulin effects in muscle and adipose tissue. *Diabetes Res Clin Pract* 93(Suppl 1):S52–S59.
15. Ben Djoudi Ouadda A, et al. (2009) Increased hepatic lipogenesis in insulin resistance and Type 2 diabetes is associated with AMPK signalling pathway up-regulation in Psammomys obesus. *Biosci Rep* 29(5):283–292.
16. Hemmings BA, Restuccia DF (2012) PI3K-PKB/Akt pathway. *Cold Spring Harb Perspect Biol* 4(9):a011189.
17. Mackenzie RW, Elliott BT (2014) Akt/PKB activation and insulin signaling: A novel insulin signaling pathway in the treatment of type 2 diabetes. *Diabetes Metab Syndr Obes* 7:55–64.
18. Du K, Herzig S, Kulkarni RN, Montminy M (2003) TRB3: A tribbles homolog that inhibits Akt/PKB activation by insulin in liver. *Science* 300(5625):1574–1577.
19. Cohen P, Frame S (2001) The renaissance of GSK3. *Nat Rev Mol Cell Biol* 2(10):769–776.
20. Manning BD, Cantley LC (2007) AKT/PKB signaling: Navigating downstream. *Cell* 129(7):1261–1274.
21. Wu D, Pan W (2010) GSK3: A multifaceted kinase in Wnt signaling. *Trends Biochem Sci* 35(3):161–168.
22. Sun T, Rodriguez M, Kim L (2009) Glycogen synthase kinase 3 in the world of cell migration. *Dev Growth Differ* 51(9):735–742.
23. Jacobs KM, et al. (2012) GSK-3β: A bifunctional role in cell death pathways. *Int J Cell Biol* 2012:930710.
24. Beurel E, Michalek SM, Jope RS (2010) Innate and adaptive immune responses regulated by glycogen synthase kinase-3 (GSK3). *Trends Immunol* 31(1):24–31.
25. McManus EJ, et al. (2005) Role that phosphorylation of GSK3 plays in insulin and Wnt signalling defined by knockin analysis. *EMBO J* 24(8):1571–1583.
26. Boini KM, Bhandaru M, Mack A, Lang F (2008) Steroid hormone release as well as renal water and electrolyte excretion of mice expressing PKB/SGK-resistant GSK3. *Pflugers Arch* 456(6):1207–1216.
27. Boini KM, Amann K, Kempe D, Alessi DR, Lang F (2009) Proteinuria in mice expressing PKB/SGK-resistant GSK3. *Am J Physiol Renal Physiol* 296(1):F153–F159.
28. Föller M, et al. (2011) PKB/SGK-resistant GSK3 enhances phosphaturia and calciuria. *J Am Soc Nephrol* 22(5):873–880.
29. Fisman EZ, Tenenbaum A (2014) Adiponectin: A manifold therapeutic target for metabolic syndrome, diabetes, and coronary disease? *Cardiovasc Diabetol* 13:103.
30. Lara-Castro C, Fu Y, Chung BH, Garvey WT (2007) Adiponectin and the metabolic syndrome: Mechanisms mediating risk for metabolic and cardiovascular disease. *Curr Opin Lipidol* 18(3):263–270.
31. Kadowaki T, et al. (2006) Adiponectin and adiponectin receptors in insulin resistance, diabetes, and the metabolic syndrome. *J Clin Invest* 116(7):1784–1792.
32. Aye IL, Rosario FJ, Powell TL, Jansson T (2015) Adiponectin supplementation in pregnant mice prevents the adverse effects of maternal obesity on placental function and fetal growth. *Proc Natl Acad Sci USA* 112(41):12858–12863.
33. Liu Q, et al. (2012) Adiponectin regulates expression of hepatic genes critical for glucose and lipid metabolism. *Proc Natl Acad Sci USA* 109(36):14568–14573.
34. Awazawa M, et al. (2011) Adiponectin enhances insulin sensitivity by increasing hepatic IRS-2 expression via a macrophage-derived IL-6-dependent pathway. *Cell Metab* 13(4):401–412.
35. Karpe F (2013) Insulin resistance by adiponectin deficiency: Is the action in skeletal muscle? *Diabetes* 62(3):701–702.
36. Qiao L, Zou C, van der Westhuyzen DR, Shao J (2008) Adiponectin reduces plasma triglyceride by increasing VLDL triglyceride catabolism. *Diabetes* 57(7):1824–1833.
37. Matsuura F, et al. (2007) Adiponectin accelerates reverse cholesterol transport by increasing high density lipoprotein assembly in the liver. *Biochem Biophys Res Commun* 358(4):1091–1095.
38. Ryo M, et al. (2004) Adiponectin as a biomarker of the metabolic syndrome. *Circ J* 68(11):975–981.
39. Gallou-Kabani C, et al. (2007) C57BL/6J and A/J mice fed a high-fat diet delineate components of metabolic syndrome. *Obesity (Silver Spring)* 15(8):1996–2005.
40. Wilson PW, Grundy SM (2003) The metabolic syndrome: A practical guide to origins and treatment: Part II. *Circulation* 108(13):1537–1540.
41. Kaur J (2014) A comprehensive review on metabolic syndrome. *Cardiol Res Pract* 2014: 943162.
42. Fu Y (2014) Adiponectin signaling and metabolic syndrome. *Prog Mol Biol Transl Sci* 121:293–319.
43. Holland WL, et al. (2013) An FGF21-adiponectin-ceramide axis controls energy expenditure and insulin action in mice. *Cell Metab* 17(5):790–797.
44. Qiao L, et al. (2005) C/EBPalpha regulates human adiponectin gene transcription through an intronic enhancer. *Diabetes* 54(6):1744–1754.
45. Ross SE, Erickson RL, Hemati N, MacDougald OA (1999) Glycogen synthase kinase 3 is an insulin-regulated C/EBPalpha kinase. *Mol Cell Biol* 19(12):8433–8441.
46. West DB, Boozer CN, Moody DL, Atkinson RL (1992) Dietary obesity in nine inbred mouse strains. *Am J Physiol* 262(6 Pt 2):R1025–R1032.
47. Diehl AM (2004) Fatty liver, hypertension, and the metabolic syndrome. *Gut* 53(7): 923–924.
48. Lonardo A, Ballestri S, Marchesini G, Angulo P, Loria P (2015) Nonalcoholic fatty liver disease: A precursor of the metabolic syndrome. *Dig Liver Dis* 47(3):181–190.
49. Wicklow BA, et al. (2012) Metabolic consequences of hepatic steatosis in overweight and obese adolescents. *Diabetes Care* 35(4):905–910.
50. Soeiro-de-Souza MG, et al. (2014) Lithium decreases plasma adiponectin levels in bipolar depression. *Neurosci Lett* 564:111–114.
51. Yadav A, Kataria MA, Saini V, Yadav A (2013) Role of leptin and adiponectin in insulin resistance. *Clin Chim Acta* 417:80–84.
52. Lihn AS, Pedersen SB, Richelsen B (2005) Adiponectin: Action, regulation and association to insulin sensitivity. *Obes Rev* 6(1):13–21.
53. Cha HC, et al. (2008) Phosphorylation of CCAAT/enhancer-binding protein alpha regulates GLUT4 expression and glucose transport in adipocytes. *J Biol Chem* 283(26): 18002–18011.
54. Ekmekci H, Ekmekci OB (2006) The role of adiponectin in atherosclerosis and thrombosis. *Clin Appl Thromb Hemost* 12(2):163–168.
55. Kizer JR (2014) Adiponectin, cardiovascular disease, and mortality: Parsing the dual prognostic implications of a complex adipokine. *Metabolism* 63(9):1079–1083.
56. Dalamaga M, Diakopoulos KN, Mantzoros CS (2012) The role of adiponectin in cancer: A review of current evidence. *Endocr Rev* 33(4):547–594.
57. Mangge H, et al. (2010) Inflammation, adiponectin, obesity and cardiovascular risk. *Curr Med Chem* 17(36):4511–4520.
58. Otvos L, Jr, et al. (2011) Design and development of a peptide-based adiponectin receptor agonist for cancer treatment. *BMC Biotechnol* 11:90.
59. Cohen P, Goedert M (2004) GSK3 inhibitors: Development and therapeutic potential. *Nat Rev Drug Discov* 3(6):479–487.
60. Kramer T, Schmidt B, Lo Monte F (2012) Small-molecule inhibitors of GSK-3: Structural insights and their application to Alzheimer's disease models. *Int J Alzheimers Dis* 2012:381029.
61. Frame S, Cohen P (2001) GSK3 takes centre stage more than 20 years after its discovery. *Biochem J* 359(Pt 1):1–16.
62. Lizcano JM, Alessi DR (2002) The insulin signalling pathway. *Curr Biol* 12(7): R236–R238.
63. Mendonça FM, et al. (2015) Metabolic syndrome and risk of cancer: Which link? *Metabolism* 64(2):182–189.
64. Yap TA, Bjerke L, Clarke PA, Workman P (2015) Drugging PI3K in cancer: Refining targets and therapeutic strategies. *Curr Opin Pharmacol* 23:98–107.
65. Li B, Thrasher JB, Terranova P (2015) Glycogen synthase kinase-3: A potential preventive target for prostate cancer management. *Urol Oncol* 33(11):456–463.
66. Beurel E, Grieco SF, Jope RS (2015) Glycogen synthase kinase-3 (GSK3): Regulation, actions, and diseases. *Pharmacol Ther* 148:114–131.
67. McCubrey JA, et al. (2014) GSK-3 as potential target for therapeutic intervention in cancer. *Oncotarget* 5(10):2881–2911.

Supporting Information

Chen et al. 10.1073/pnas.1601355113

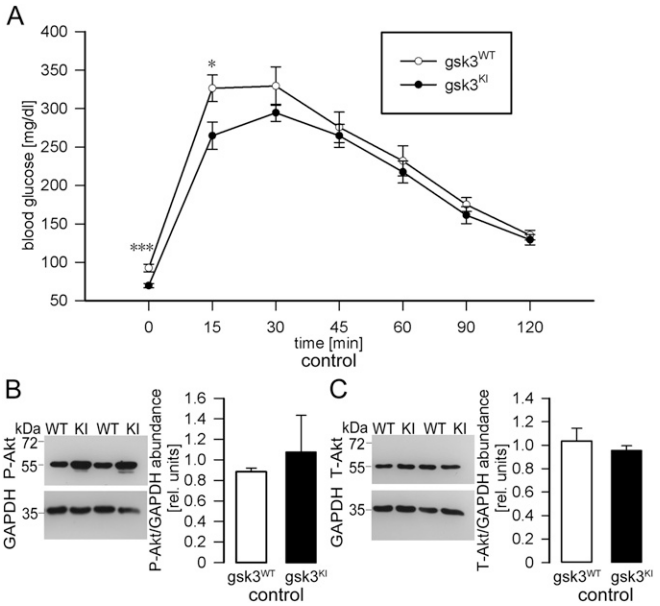

Fig. S1. Glucose tolerance test and insulin-induced Akt phosphorylation in gsk-3^{WT} and gsk-3^{KI} mice fed a control diet. (*A*) Arithmetic means ± SEM of blood glucose concentration (n = 9–11) following i.p. injection of glucose (2 g/kg body weight) into 6- to 8-wk-old gsk3^{WT} and gsk3^{KI} mice fed a control diet. The glucose tolerance test of another group of mice after 10 wk of feeding a high-fat diet is shown in Fig. 3*B*. (*B* and *C*) Original Western blots (*Left* panels) demonstrating the abundance of P-Akt (Thr308, *B*) and of total Akt (*C*) in livers isolated from 5- to 6-mo-old gsk3^{WT} and gsk3^{KI} mice fed a control diet 8 min after insulin injection (0.5 U/kg body weight). GAPDH expression is also shown. (*Right* panels) Densitometric analysis (arithmetic means ± SEM; n = 4); white bar: gsk3^{WT} mice; black bar: gsk3^{KI} mice., *P < 0.05 and ***P < 0.001 indicate significant difference from gsk3^{WT} mice.

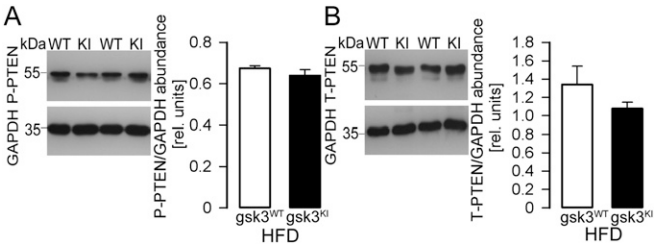

Fig. S2. PTEN activity in livers from high-fat-diet–fed gsk-3^{WT} and gsk-3^{KI} mice. Original Western blots demonstrating (*A*) P-PTEN (Ser380/Thr382/383) and (*B*) total PTEN abundance in livers from gsk-3^{WT} mice and gsk-3^{KI} mice after 12 wk of feeding a high-fat diet. For both blots, GAPDH expression is also shown. (*Right* panels) The densitometric analysis (arithmetic means ± SEM; n = 4); white bars: gsk3^{WT} mice; black bars: gsk3^{KI} mice.